**Proceedings of the XVII ECSMGE-2019**
Geotechnical Engineering foundation of the future
ISBN 978-9935-9436-1-3

doi: 10.32075/17ECSMGE-2019-0177

XVII European Conference
ECSMGE 2019
Reykjavik
on Soil Mechanics
and Geotechnical Engineering

# Centrifuge study on the effect of pile location on the slope stabilized by piles

## L'Etude par centrifugation de l'effet de la localisation des pieux sur la pente stabilisée par pieux

G. Lei
*Institute of Geotechnical Engineering, University of Natural Resources and Life Sciences, Vienna, Austria*

W. Wu
*Institute of Geotechnical Engineering, University of Natural Resources and Life Sciences, Vienna, Austria*

**ABSTRACT:** Piles arranged in rows are widely used for slope stabilization. The location of the piles is one of the decisive factors for a reliable pile reinforcement. In this paper, the effect of pile location is studied by centrifuge model tests. The piles are installed in a row to stabilize a slope with an inclination of 45°. The slope movement is monitored by a digital camera pointing to the model side. Strain gauges are installed on the pile to obtain the bending moment. The effect of the pile location is studied by increasing the up-slope length. As the relative pile location moves towards the slope toe, larger soil displacement and higher soil pressure on the pile are obtained. The slope failure mode changes from the down-slope failure to the over-top failure.

**RÉSUMÉ:** Les pieux disposés en rangées sont largement utilisés pour la stabilisation des pentes. L'emplacement des pieux est l'un des facteurs décisifs pour un renforcement fiable des pieux. Dans cet article, l'effet de l'emplacement des pieux est étudié par des essais sur modèle centrifuge. Les pieux sont installés en rangée pour stabiliser une pente avec une inclinaison de 45°. Le mouvement de la pente est surveillé par une caméra numérique pointant vers le côté du modèle. Des jauges de contrainte sont installées sur le pieu pour obtenir le moment de flexion. L'effet de l'emplacement du pieu est étudié en augmentant la longueur de la pente ascendante. Lorsque l'emplacement relatif du pieu se déplace vers le pied de la pente, on obtient un déplacement plus important du sol et une pression accrue du sol sur le pieu. Le mode de rupture de pente passe de la défaillance en descente à la défaillance au sommet.

**Keywords:** Pile location; slope stabilization; centrifuge test

## 1 INTRODUCTION

Stabilizing piles have been extensively applied over the past few decades to increase slope stability. The first step of the pile design is usually the determination of pile location in the slope, which is the optimum of two considerations. The first one is the strength of stable soil, in which the piles are embedded. The optimal pile location should provide the maximum stable soil strength so that the pile embedded length is minimized. A case of stabilizing piles in colluvial

landslide has been studied by Li et al. (2017) where the optimal pile location is determined according to the combination of hard and soft bedrocks. The second consideration is the effectiveness of piles. Intensive pile-soil interaction and large soil pressure on pile should be mobilized. Based on an analytical method, Wang and Yen (1974) concluded that the necessary slope length to develop the soil arching fully is approximately 5-6 times the pile spacing. The traditional limit equilibrium methods were modified by many researchers to calculate the slope stability considering the effect of piles (Lee et al., 1995; Hassiotis et al., 1997; Jeong et al., 2003; Zhang and Wang, 2010; Yamin and Liang, 2010; Ashour and Ardalan, 2012). The optimal pile location can be determined according to the variation of slope stability with pile location. These studies conclude that the piles are best placed near the mid-slope, which is also confirmed by numerical analysis (Ellis et al., 2010). However, these methods do not consider the variation of slip surface or the appearance of secondary slip surface due to the installation of piles. Centrifuge model test is closer to the reality when soil deformation and failure are concerned. Wang and Zhang (2014) observed from centrifuge tests that the slope deformation behaviour is significantly affected by the pile location. Yoon and Ellis (2009) concluded from centrifuge tests that the soil-pile contacting force increases with the up-slope length. However, the failure modes were not well revealed in their tests.

In this study, centrifuge tests of an unstable slope reinforced by a row of piles are reported. The effect of pile location is considered by changing the up-slope length. In-flight photography and Particle Image Velocimetry (PIV) are adopted to measure the soil movements. Pile deformation is measured by strain gauge instrumentation. It is observed that as the up-slope increases, which is equivalent to moving the piles towards the slope toe, the soil pressure on pile increases and the failure mode changes from down-slope failure to over-top failure.

## 2 CENTRIFUGE MODELLING

The centrifuge tests were performed on the geotechnical beam centrifuge at the University of Natural Resources and Life Sciences, Vienna. Figure 1 shows the model geometry in the side-view. The 45° slope is reinforced by a row of discrete piles with a pile spacing/diameter ratio of 3.10. The effect of pile location is considered by changing the up-slope length $l$. As shown in Figure 1, three cases are considered: lines L ($l/l_s$=0.59), M ($l/l_s$=0.48) and S ($l/l_s$=0.33) denote the crest for long, middle and short slopes, respectively. From model S to L, the relative pile location has moved from the upper half-slope to somewhere lower that the mid-slope.

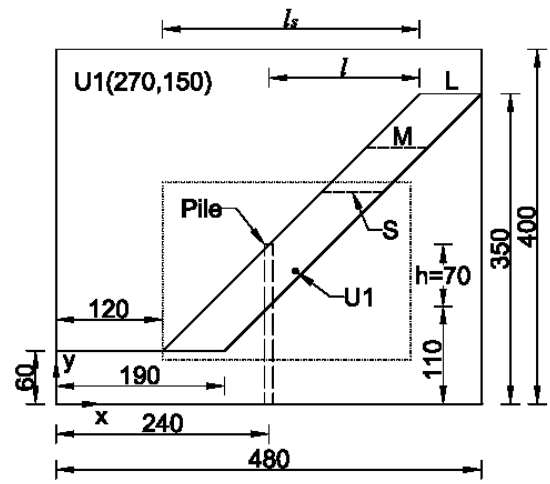


*Figure 1. Model geometry in the cross-sectional view (unit: mm).*

### 2.1 Model construction

The slope consists of two layers: a sliding soil layer and a stationary layer underneath modelled by wood. A slip surface with low friction is installed between these two layers using a 2 mm thick rubber sheet with smooth surface and a 1 mm thick aluminium sheet with sprayed silicon oil in between. The aluminium sheet is attached to the surface of the stable layer and the rubber

sheet is attached to the bottom of the soil layer. The pile top and toe line up with the ground surface and the bottom of the wooden structure, respectively. The total length of the model pile is 18 cm with an embedded length of 11 cm. After the construction of the stable layer, the installation of the slip surface as well as the placement of model piles, the premixed soil sample is compacted to the required density via moist tamping. Divided horizontal sub-layers with the thickness of 25 mm are found to be adequate to produce a uniform density distribution in the soil. After the compaction, the soil is cut to the designed model dimensions.

## *2.2* Materials

The model piles are made of aluminium tube with a wall thickness of 1 mm. The pile diameter is 10mm and the bending stiffness is 18.21 $MNmm^2$. The model soil is medium-fine sand with a minor fraction of silt. The relative density $D_r$ of the soil sample used for all the experiments is 0.55 which lies in the range of medium dense. The corresponding dry density $\rho_d$ and void ratio $e$ are 1.53 $g/cm^3$ and 0.74, respectively. For each test the soil sample is prepared with a water content of 11.5%. According to the drained triaxial tests, the effective internal frictional angle $\phi'$ is 31.8° and the cohesion $c$ is 6.0 kPa.

## *2.3* Instrumentations

A digital camera is used to take images of the side of the model slope to track the in-plane soil displacement using the technique of Particle Image Velocimetry (PIV) provided by the Matlab code GeoPIV (White et al., 2003). The dotted rectangle in Figure 1 indicates the area where PIV analysis is applied in the side-view. 8 pairs of strain gauges are installed on the pile to monitor the bending moment. Figure 2 shows the distribution of strain gauges along the pile. The measured bending moments are further fitted to estimate the soil pressure on the pile.

## *2.4* G-up procedure

The only triggering factor for the soil movement is gravity. A g-up test procedure with an increasing rate of 0.1 per second for the centrifugal acceleration (rpm) is employed, continuously increasing the gravity-induced stress field. The increase of stresses in the model slope corresponds to the increase of the prototype slope height. The designed maximum g-level is 50.

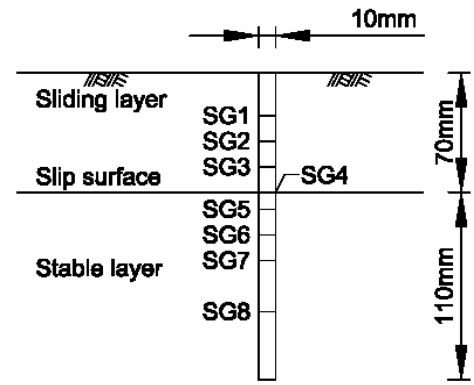


*Figure 2. Strain gauge distribution along the pile.*

# 3 RESULTS AND ANALYSIS

The measured soil displacement is used to reveal the influence of relative pile location. The soil pressure on the pile, which is derived from bending moment measurements of the pile, is also analysed.

## *3.1* Soil displacement analysis

U1 (see Figure 1) is a monitoring point which is used to represent the movement of the soil layer). The soil displacement at U1 is plotted against g-level in Figure 3. It shows that the U1 displacement is less than 10 mm and it is not influenced by the increase of up-slope length. This is because the point U1 is located in the soil zone that is directly stabilised by the pile row. The additional soil in the up-slope only accelerates the movement of the soil part that can move

above the pile top, which will be proved by the soil displacement distribution in the whole layer. This also implies that the support of the pile row to the up-slope soil with this spacing/diameter ratio (3.10) is solid.

Figure 4, 5 and 6 show the soil displacement of the side-view at 50 g for model S, M and L, respectively. The soil displacement in the up-slope increases with $l/l_s$. Displacement discontinuity is observed at the pile row. In the case of model S, the soil displacement in the down-slope is much larger than the up-slope, therefore this test is prone to 'down-slope failure'. In the case of model L, the large soil displacement concentrates only in the up-slope with the altitude higher that the pile top, which indicates the 'over-top failure'. In the case of model M, the signs of both failure modes can be seen.

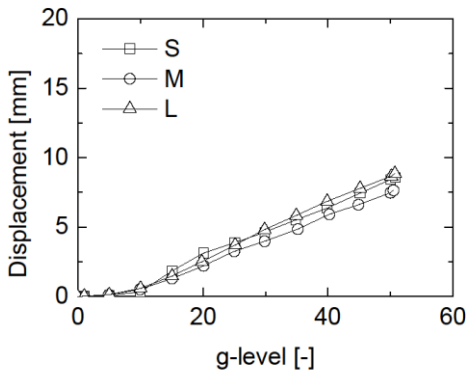


*Figure 3. PIV computed U1 displacement.*

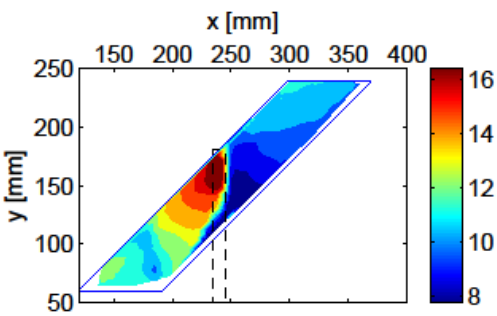


*Figure 4. Soil displacement (unit:mm) at 50 g in the side-view for Model S ($l/l_s$=0.33).*

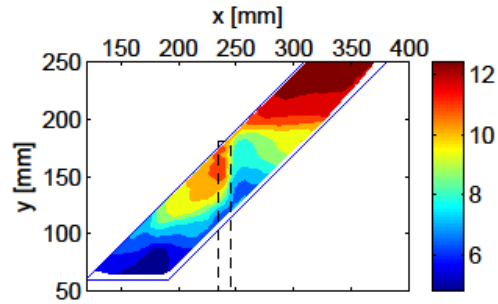


*Figure 5. Soil displacement (unit:mm) at 50 g in the side-view for Model M ($l/l_s$=0.48).*

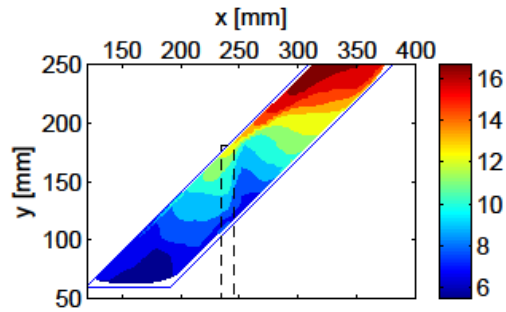


*Figure 6. Soil displacement (unit:mm) at 50 g in the side-view for Model L ($l/l_s$=0.59).*

## *3.2* Soil deformation analysis

The observations of displacement are further verified by the soil deformation. Figure 7, 8 and 9 show the PIV computed maximum shear strain of the side-view for model S, M and L, respectively. The soil strain in the slope toe area is caused by the sudden change of slip surface inclination and is, therefore, neglected here. For model S, a vertical shear band is observed at the pile row, indicating a down-slope failure. As $l/l_s$ increases, an inclined shear band starting at the pile top and extending to the up-slope appears and becomes the main deformation in the soil layer. The tendency of over-top failure is well revealed in Figure 9.

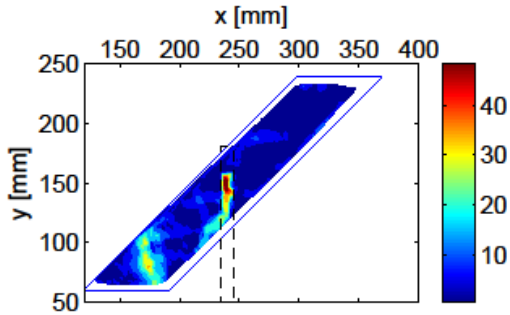


*Figure 7. Maximum shear strain (%) at 40 g in the side-view for Model S ($l/l_s$=0.33).*

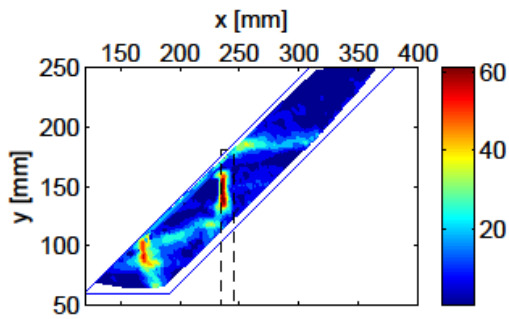


*Figure 8. Maximum shear strain (%) at 50 g in the side-view for Model M ($l/l_s$=0.48).*

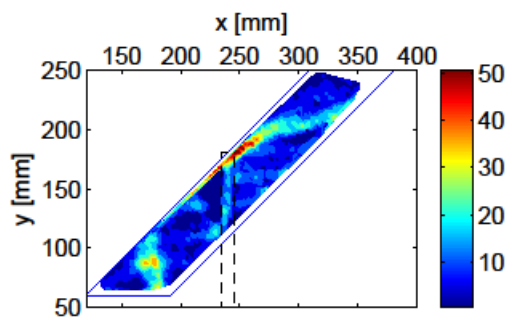


*Figure 9. Maximum shear strain (%) at 45 g in the side-view for Model L ($l/l_s$=0.59).*

## *3.3* Soil pressure on the pile

The soil pressure on pile is derived from the bending moment measurements. A non-dimensional parameter is used to describe the stress level:

$$B_{mob} = \frac{p}{\sigma'_{v0}} \tag{1}$$

Where $p$ is the soil pressure on pile and $\sigma'_{v0}$ is the overburden pressure at the same depth.

The value of $B_{mob}$ at the middle of the soil layer is chosen to make comparisons because it is less affected by the layer boundaries. The increase of $B_{mob}$ with g-level is plotted in Figure 10. At large g-level, all the $B_{mob}$ values become stable and independent of the g-level, indicating a stable pile-soil interaction. From model S to model L, the stable $B_{mob}$ has increased. However, the increasing rate of $B_{mob}$ (99%) is much smaller than the increasing rate of the up-slope length $l$ (187%) from model S to model L. The reason for that is the appearance of over-top failure when the piles move relatively to the slope toe.

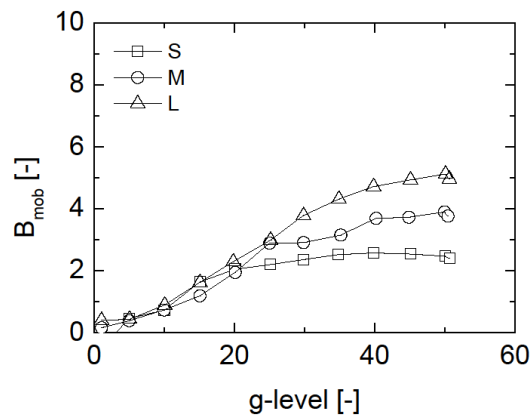


*Figure 10. Increase of the normalised soil pressure with g-level.*

## 4 CONCLUSIONS

This study reports a series of centrifuge model tests investigating the effect of pile location on the slope stabilized by piles. In each centrifuge test, the unstable slope was simulated by a 45° inclined soil layer sliding on a stable wood structure with a smooth sliding surface in between. The effect of pile location is considered by changing the up-slope length. Based on the analyses of the displacement and pile bending measurements, the following conclusions can be drawn: The relative pile location $l/l_s$ has a large influence on the slope failure mode. By moving the relative pile location towards the slope toe ($l/l_s$ increases from 0.33 to 0.59), larger soil displacement in the up-slope and soil pressure on the pile are obtained. The failure mode changes from down-slope failure to over-top failure. The appearance of over-top failure has reduced the increasing rate of soil pressure on pile.

## 5 ACKNOWLEDGEMENTS

The authors wish to acknowledge the financial support from China Scholarship Council (No. 201306410004), Otto Pregl Foundation for Fundamental Geotechnical Research in Vienna, as well as H2020 Marie Skłodowska-Curie Actions RISE 2014 'Geo-ramp' (grant number 645665).

## 6 REFERENCES

Ashour, M., & Ardalan, H. (2012). Analysis of pile stabilized slopes based on soil–pile interaction. Computers and Geotechnics, 39, 85-97.

Ellis, E. A., Durrani, I. K., & Reddish, D. J. (2010). Numerical modelling of discrete pile rows for slope stability and generic guidance for design. Geotechnique, 60(3), 185.

Hassiotis, S., Chameau, J. L., & Gunaratne, M. (1997). Design method for stabilization of slopes with piles. Journal of Geotechnical and Geoenvironmental Engineering, 123(4), 314-323.

Jeong, S., Kim, B., Won, J., & Lee, J. (2003). Uncoupled analysis of stabilizing piles in weathered slopes. Computers and Geotechnics, 30(8), 671-682.

Lee, C. Y., Hull, T. S., & Poulos, H. G. (1995). Simplified pile-slope stability analysis. Computers and Geotechnics, 17(1), 1-16.

Li, C., Wang, X., Tang, H., Lei, G., Yan, J., & Zhang, Y. (2017). A preliminary study on the location of the stabilizing piles for colluvial landslides with interbedding hard and soft bedrocks. Engineering Geology, 224, 15-28.

Wang, W. L., & Yen, B. C. (1974). Soil arching in slopes. Journal of Geotechnical Engineering, 100(gt1).

Wang, L. P., & Zhang, G. (2014). Progressive failure behavior of pile-reinforced clay slopes under surface load conditions. Environmental earth sciences, 71(12), 5007-5016.

White, D. J., Take, W. A., & Bolton, M. D. (2003). Soil deformation measurement using particle image velocimetry (PIV) and photogrammetry. Geotechnique, 53(7), 619-631.

Yamin, M., & Liang, R. Y. (2010). Limiting equilibrium method for slope/drilled shaft system. International Journal for Numerical and Analytical Methods in Geomechanics, 34(10), 1063-1075.

Yoon, B. S., & Ellis, E. A. (2009). Centrifuge modelling of slope stabilisation using a discrete pile row. Geomechanics and Geoengineering: An International Journal, 4(2), 103-108.

Zhang, G., & Wang, L. (2010). Stability analysis of strain-softening slope reinforced with stabilizing piles. Journal of geotechnical and geoenvironmental engineering, 136(11), 1578-1582.